



## Electroplating of copper onto a preanodized 7005Al/Al<sub>2</sub>O<sub>3(P)</sub> metal matrix composite

J-C. LIN\*, W-D. JEHNG and S-L. LEE

Department of Mechanical Engineering, National Central University, No. 300, Chung Ta Road, Chung-Li, Taiwan 320, Republic of China

(\*author for correspondence, fax: +886 3 4254501, e-mail: jclincom@rs250.ncu.edu.tw)

Received 19 November 2002; accepted in revised form 3 March 2003

*Key words:* anodizing, copper plating, electrochemical methods, metal matrix composites

### Abstract

The electroplating of copper onto 7005Al/Al<sub>2</sub>O<sub>3(P)</sub> metal matrix composites (Al MMC) is difficult but becomes feasible if the composites have been preanodized in mineral acids. It is clear that phosphoric (P) acid anodizing is better than oxalic (O) or sulfuric (S) acid anodizing when the morphology of the copper coating and its adhesion to the MMC substrate are considered. Electrochemical studies, such as cyclic anodic potentiodynamic polarization (CAPP), cyclic cathodic potentiodynamic polarization (CCPP) and electrochemical impedance spectroscopy (EIS) are beneficial in delineating the influence of the anodizing pretreatment on the subsequent copper electroplating process. A positive hysteresis of the CAPP curve in phosphoric acid indicates the effective removal of oxide film from the composite. After examining the CCPP curves for the Cu-electroplating bath, for MMC pretreated in various acids, we can understand the morphological differences in the copper coatings and variations in adhesion to the anodized composite. EIS measurements confirm the d.c.-polarization results.

### 1. Introduction

Aluminium matrix composites (Al MMCs) can consist of continuous or discontinuous reinforced phases (e.g., fibres, whiskers or particles of carbon, graphite, boron, alumina and silicon carbide) in an aluminium alloy matrix [1–3]. The addition of reinforcement phases strengthen the aluminium alloys. These Al MMCs are considered to be good engineering materials because of their high strength to weight ratio, high specific modulus and unique combination of several tailored properties. However, the use of reinforcement phases with ordinarily cause a sacrifice of metal luster and hardness homogeneity. Electroplating is considered one of the ways to compensate for these drawbacks.

Ordinarily, during industrial finishing, successive layers of electroplating, such as copper, nickel and chromium, are applied [4]. In this Cu–Ni–Cr multilayer system, copper acts as the undercoating for levelling, nickel as the anticorrosion sublayer, and chromium acts as the antiwear topcoat. Even though the use of copper may lead to galvanic corrosion, it is still considered to be an excellent undercoating for the following reasons: (i) it is feasible to use for electroplating onto a variety of metals; (ii) satisfactory throwing power which leads to uniform coverage; (iii) good coherence of subsequent coats. Accordingly, an attempt to electroplate successive

Cu–Ni–Cr layers onto Al MMC was made which, unfortunately, failed during the first stage, where we tried to electroplate a copper undercoating directly onto the surface of a 7005Al/Al<sub>2</sub>O<sub>3(P)</sub> MMC specimen.

Al MMC electroplating has seldom been reported [5, 6]. However, a few instances of successful metal electroplating onto aluminium alloys have been discussed [7, 8]. Although the feasibility of the process has been subject to discussion [9–12], it is generally agreed that the difficulty of electroplating onto aluminium alloys can be ascribed to the hindrance of an intrinsic oxide film that adheres tightly to the aluminium surface. This film can be diminished by means of pretreatments, such as (i) the immersion of Al-alloys in either a zincate or stannate solution; (ii) the anodizing of the Al-alloy samples in acid solutions before electroplating.

In preliminary tests, we found an anodizing pretreatment to be preferable to zincate (or stannate) immersion for a good subsequent copper coat. The morphology of the Cu-coating and its adhesion to the Al MMC substrate varied with the type of bath chosen for preanodizing. The electrochemical behaviour of the composite samples anodized in phosphoric, oxalic and sulfuric acids is of particular interest in this work. The feasibility of copper electroplating is discussed on the basis of the cathodic behaviour of Al MMC samples preanodized in copper sulfate.

## 2. Experimental details

Particles of aluminium oxide, roughly 1–3  $\mu\text{m}$  in diameter, were well dispersed at 15 percent of the volume in a Al 7005 alloy melt to produce 7005Al/Al<sub>2</sub>O<sub>3(p)</sub> MMC. The composition (wt %) of the Al 7005 alloy was 4.73 Zn, 1.68 Mg, 0.46 Fe, 0.35 Si, 0.23 Mn, 0.18 Cu, 0.17 Cr, 0.03 Ti and Bal. Al. Al MMC ingots, (50 mm  $\times$  80 mm  $\times$  200 mm) were cast from the molten mixture, then sliced into rectangular specimens (60 mm  $\times$  30 mm  $\times$  2 mm). The specimens were ground mechanically with a series of abrasive papers (600–1200 grit), then chemically polished in a solution of mixed acids (4.2 M H<sub>3</sub>PO<sub>4</sub> + 1.2 M CH<sub>3</sub>COOH + 0.4 M HNO<sub>3</sub>) at 25 °C for 60 s, then rinsed in bidistilled water and dried.

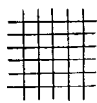

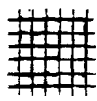


The chemically polished specimens were anodized in an acid solution (0.500  $\times 10^{-3}$  m<sup>3</sup>) at 1,200 V, against a saturated calomel electrode (SCE), for 1 h. Oxalic, phosphoric and sulfuric acids, respectively, were employed as electrolytes in the different anodizing treatments. A plate of high density graphite was used as the auxiliary electrode (i.e., cathode) and a potentiostat (Hokuto Denko, HA320) was used as the d.c. power supply. The temperature of the baths was controlled at 25  $\pm$  1 °C.

The decreasing current range for the copper electroplating process was estimated from the results of a series of copper electroplating procedures conducted in a Hull cell [13]. An acidic copper sulfate solution (0.84 M CuSO<sub>4</sub> + 0.51 M H<sub>2</sub>SO<sub>4</sub>) at a temperature of 25 °C was used as the electrolyte source, for the Hull cell test, with an applied voltage of 0.35–0.5 V. Sheets of Al MMC that had been preanodized in various acids were used as the cathodes, and sheets of pure copper (99.99%) as the anodes. The electroplating d.c. current was supplied by a potentiostat. The Cu-deposits were rinsed with bidistilled water and dried before their morphology was examined with through an optical microscope (OM, Olympus-BX60M) and a scanning electron microscope (SEM, Hitachi S-2500).

The adhesion of the copper coating to the preanodized Al MMC substrate was measured by a tape test, using the standard ASTM method, D3359. The coating was first cut through to the substrate by a cutting tool (ten razor blades). Additional cuts were made at 90 degrees to form a grid of 100 spaces. A one-inch wide piece of semitransparent pressure-sensitive tape (3M™ paper masking tape 2214) with a adhesion strength of 40 g mm<sup>-1</sup>, was placed on the grids to ensure good contact. The tape was then pulled off and the area inspected. The adhesion strength of the coat to the substrate was classified into six levels, which are listed in Table 1. Copper coatings with adhesion strengths in classes 0 or 1 were classified as satisfactory, so their corresponding electroplating processes are recommended.

Cyclic potentiodynamic polarization was conducted in a standard electrochemical cell using a platinized titanium counter electrode, and using an SCE (saturated calomel electrode) with a Luggin probe as the reference

Table 1. Classification of adhesion test results (ASTM D3359)

Class	Description	Surface
0	Edges of the cuts are complete smooth; none of the squares of the lattice is detached.	
1	Small flakes of the coating are detached at intersections; less than 5% of the area is affected.	
2	Small flakes of the coating are detached along edges and at intersections of cut. Area affected is 5% to 35% of the lattice.	
3	Coating has flakes along the edges and on parts of the squares. Area affected is 15% to 35% of the lattice.	
4	Coating has flakes along the edges of the cuts in large ribbons and whole squares have detached. Area affected is 35% to 65% of the lattice.	
5	Flaking and detachment worse than grade 4.	

electrode. All potentials were related to the SCE. Chemically polished specimens were used as working electrodes to obtain cyclic anodic potentiodynamic polarization (CAPP) curves in the various acid solutions. As well preanodized specimens were used as the working electrodes to obtain cyclic cathodic potentiodynamic polarization (CCPP) curves in the copper sulfate solution. The specimens were coated with epoxy resin heaving an area of 100 mm<sup>2</sup> exposed. The working and counter electrodes were separated by 40 mm. A cyclic voltammeter (Bioanalytical Systems, BAS-100B) was employed to conduct the cyclic voltammetry, at a scan rate of 10 mV s<sup>-1</sup>. The potential scan was set from  $E_{\text{rest}} - 0.50$  V, to  $E_{\text{rest}} + 2.50$  V, then back to  $E_{\text{rest}}$  for the CAPP; and from  $E_{\text{rest}} + 0.1$  V, to  $E_{\text{rest}} - 1.5$  V, and back to  $E_{\text{rest}}$ , for the CCPP.  $E_{\text{rest}}$  indicates the open circuit potential (OCP). The same electrochemical cell was used for the electrochemical impedance spectroscopy (EIS). An impedance spectrometer (EG&G PARC, model 6310) was employed with M398 software. EIS was performed on preanodized specimens immersed in copper sulfate electrolyte solution. A perturbation of  $\pm 5$  mV on the OCP within a frequency range of 10<sup>-2</sup>–10<sup>5</sup> Hz was used.

## 3. Results

### 3.1. Adhesive strength of copper coats on MMC substrates preanodized in various acid solutions

Table 2 indicates that the adhesion strength varied with the pretreatment bath. As mentioned earlier, copper

Table 2. Variation of the adhesion levels (defined in Table 1) with the anodizing bath and its concentration

Type of anodizing bath	Acid concentration /M						
	0.25	0.5	1.0	2.0	3.0	4.0	4.5
Phosphoric acid	3	2	2	1	0	1	2
Oxalic acid	1	0	2	2	3	4	4
Sulfuric acid	3	2	1	2	3	4	4

deposits with an adhesion strength within classes 0 and 1 were considered satisfactory and thus their corresponding electroplating processes would be acceptable. Obviously, the composite samples there were pretreated in 2.0–4.0 M phosphoric acid (P), 0.25–0.5 M oxalic acid (O) and 1.0 M sulfuric acid (S) solutions all qualified for subsequent copper electroplating. Moreover, the best choice of anodizing pretreatment bath was phosphoric acid (P); the concentration range was wider than for the other acids, and copper coatings with stronger adhesion could be attained.

### 3.2. Copper coatings on MMC substrates preanodized in various acid solutions

The Hull cell test results indicate that the depict that copper electroplating process became feasible if the Al MMC specimens were preanodized in phosphoric, oxalic or sulfuric acid solutions in the conditions cited above. The composites that were preanodized in various acids were then subjected to copper electroplating for confirmation of the optimal operational conditions. The range of current densities used for the Cu-electroplating was wide (50–120 A m<sup>-2</sup>) for Al MMC specimens preanodized in phosphoric acid (P), medium (60–100 A m<sup>-2</sup>) for those preanodized in oxalic acid (O), and narrow (90–100 A m<sup>-2</sup>) for those preanodized in sulfuric acid (S). Obviously, the Cu-electroplating of Al MMC specimens preanodized in phosphoric acid was more feasible (i.e., a wide range of current densities could be used) than Al MMC specimens preanodized in the other acids.

Figure 1 shows the morphology of copper coatings on MMC substrates preanodized in various acids, at 1.200 V for 1 h. After electroplating at 90 A m<sup>-2</sup> for 0.25 h, a fine-grained Cu-deposit was obtained on the MMC specimens preanodized in a 3.0 M phosphoric acid solution (Figure 1(a)), a medium-nodular type of Cu-deposit on the MMC specimens preanodized in a 0.5 M oxalic acid solution (Figure 1(b)), and a large-nodular type of Cu-deposit on the MMC specimens preanodized in a 1.0 M sulfuric acid solution (Figure 1(c)). Obviously, the morphology of the copper coat was governed by the choice of preanodizing bath. According to previous work [14], the copper deposition shown in Figure 1(a) is better than that in Figure 1(b) and (c), as an undercoat for the Cu–Ni–Cr finishing on the Al MMC substrates.

### 3.3. CAPP results for the Al MMC in various anodizing acids

Figure 2 shows the CAPP curves for Al MMC specimens immersed in 0.5 M oxalic acid bath (curve O), a 1.0 M sulfuric acid bath (curve S) and a 3.0 M phosphoric acid bath (curve P), respectively. The corrosion current density has the order O < S < P at the open circuit potential (OCP). In terms of dealing with the anodizing of Al MMC substrates, the anodic polarization curves can be used to realize the anodic behavior of the aluminum in the various baths [15].

In Figure 2, curves O and P show a single hysteresis loop, but curve S is more complicate. Curve P has positive hysteresis, as the reverse scan current density is greater than the forward scan density. On the other hand, curve O has negative hysteresis as the reverse scan current density is less than the forward scan density. According to Tait [16, 17], positive hysteresis occurs when the damage in passive film is not repaired and /or pits are initiated; negative hysteresis occurs when the passive film repairs itself and pits are not initiated. In other words, the passive film on the surface of the Al MMC specimen was destroyed by the phosphoric acid bath, but it was repaired by the oxalic acid bath. The deterioration or repair of a passive film in a sulfuric acid bath depended upon the potentials applied, repair occurred only for extreme potentials (less than 0.20 or greater than 1.58 V). With respect to the anodic current density, Figure 2 shows the current curve P current to be greater than the S and O curve currents at potential between 0.2–1.2 V, in both the forward and reverse scans. This indicates that the anodic dissolution of the Al MMC specimens in the potential range 0.2–1.2 V was more pronounced in P than in S or O.

The effect of the phosphoric acid concentration on the CAPP curves was also explored. It was found that the hysteresis shifted to the right as the concentration increased. The net current density, calculated by subtracting the forward scan current density from that on the reverse scan, at constant potentials, is useful for estimating the deterioration of passive films. A positive hysteresis loop leads to a positive net current density (e.g., in phosphoric acid), while a negative hysteresis results in negative net current density (e.g., in oxalic acid). This fact, corresponding to positive net current density for P, implies that the rate of film-deterioration is greater than that of film-repairing. The magnitude of the net current density increased to a maximum when

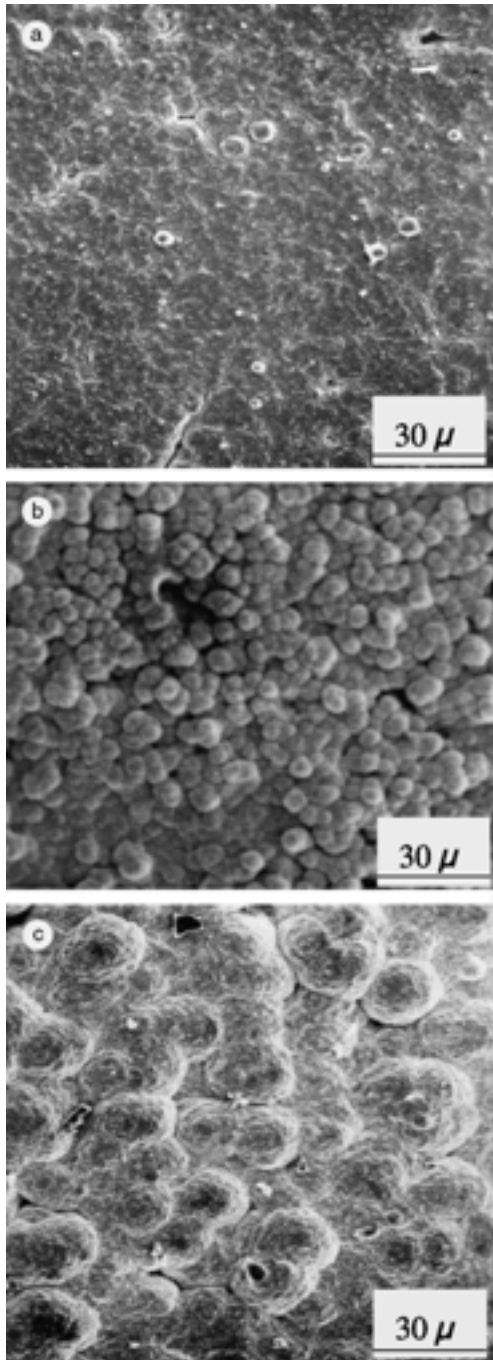


Fig. 1. SEM morphologies for the best copper coating obtained from specimens formerly anodized in (a) 3.0 M phosphoric acid, (b) 0.5 M oxalic acid and (c) 1.0 M sulfuric acid. Copper plating was conducted at  $90 \text{ A m}^{-2}$  for 0.25 h.

the phosphoric acid concentration increased from 0.5 to 3.0 M; it decreased with further increases in the acid concentration. The deterioration of the passive film on the Al MMC substrate was most severe for the 3.0 M phosphoric acid bath.

#### 3.4. SEM morphologies of Al MMC substrates anodized in various acids

Figure 3 depicts the SEM morphologies for specimens anodized at 1.20 V in various acids. The morphology of

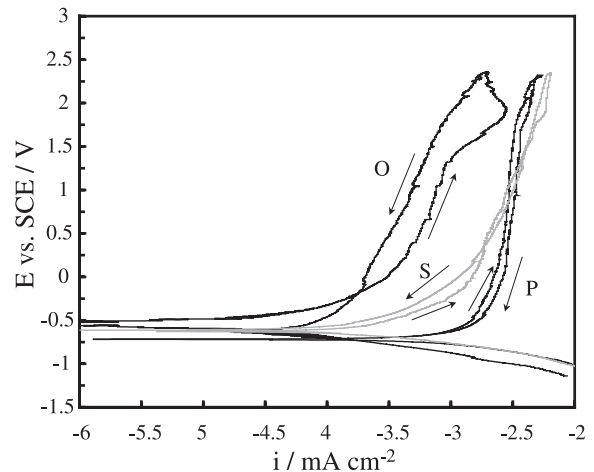


Fig. 2. Cyclic anodic potentiodynamic polarization (CAPP) curves for the specimens immersed in 3.0 M phosphoric acid (curve P), 0.5 M oxalic acid (curve O), and 1.0 M sulfuric acid (curve S).

specimens anodized in a 3.0 M phosphoric acid bath (Figure 3(a)) shows more obvious corrosion around the boundaries of the reinforcing particles. This boundary attack was also found in the composite pretreated in a 0.5 M oxalic acid solution (Figure 3(b)) and a 1.0 M sulfuric acid solution (Figure 3(c)). In addition to the boundary attack, Figure 3(a) shows some shallow pits, but Figure 3(c) shows a wrinkled film on the metal matrix. No such a wrinkled film is found in Figure 3(a) and (b).

The attack around the boundary of reinforcing particles becomes more severe with increasing anodizing acid concentrations. Beyond the critical concentrations (e.g.,  $P > 5 \text{ M}$ ,  $O > 2 \text{ M}$ , and  $S > 2 \text{ M}$ ), many reinforcing particles are excavated, leaving behind voids on the composite matrix surface. Therefore, the anodizing of the MMC specimens in concentrated acids produces no profit in terms of obtaining a smooth surface.

#### 3.5. CCPP of specimens preanodized in a copper electroplating bath

Figure 4 depicts the CCPP curves taken in the copper sulfate solution for specimens preanodized in a 0.5 M oxalic acid solution (curve O), a 3.0 M phosphoric acid solution (curve P) and a 1.0 M sulfuric acid solution (curve S). The cathodic current on the forward scans rises steeply from zero at the decomposition potential (DP), responsible for the commencement of copper electroplating [18, 19]. The less negative the DP, the easier the copper plating. In Figure 4, the DP decreases in the following order:  $P (-0.100 \text{ V}) > O (-0.110 \text{ V}) > S (-0.187 \text{ V})$ . This implies that the electroplating of copper onto Al MMC samples preanodized in phosphoric acid is easier than onto samples preanodized in oxalic or sulfuric acids.

An examination of the CCPP curves at potentials more negative than the DP, indicates that the current increases with more negative potentials. The magnitude of the

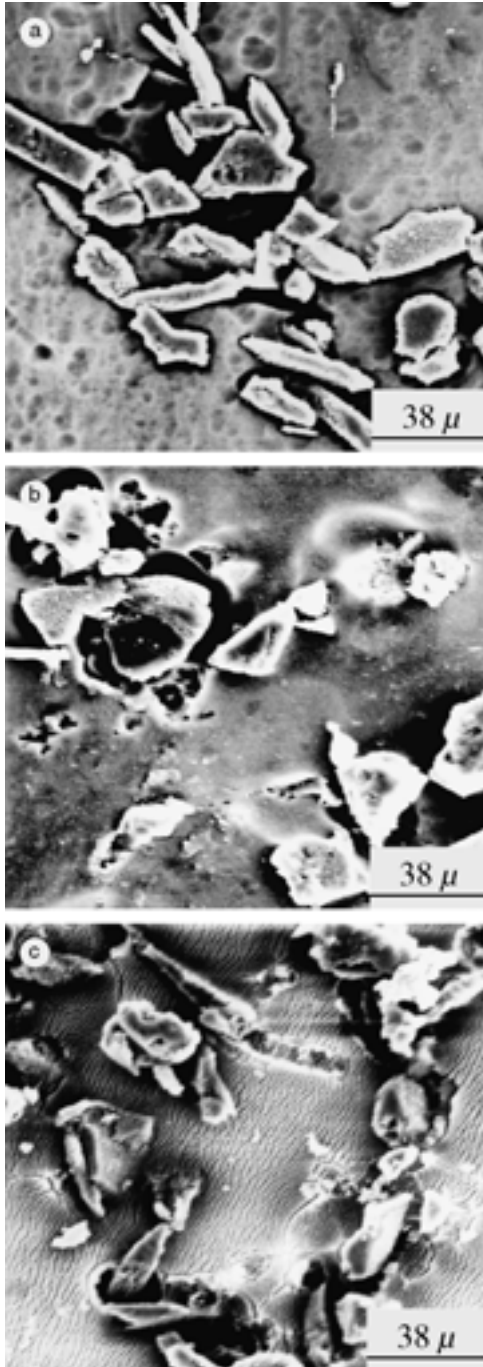


Fig. 3. SEM morphologies for 7005Al/Al<sub>2</sub>O<sub>3(P)</sub> MMC having been anodized at 1.20 V in (a) 3.0 M phosphoric acid, (b) 0.5 M oxalic acid and (c) 1.0 M sulfuric acid solutions for 1 h.

current density reflects the electrochemical reaction rate [18, 19]. As shown in Figure 4, at potentials ranging from DP to  $-0.600$  V, the current density decreases in the following order  $P > O > S$ . Thus, the rate of Cu-plating onto a Al MMC substrate preanodized in phosphoric acid is faster than for specimens that preanodized in oxalic or sulfuric acids. A satisfactory copper deposit is obtained when the preanodized specimen is put into a copper sulfate bath at potentials ranging from  $-0.300$  to  $-0.500$  V. The electroplating of copper is not practical at potentials beyond the range  $> -0.300$  V,

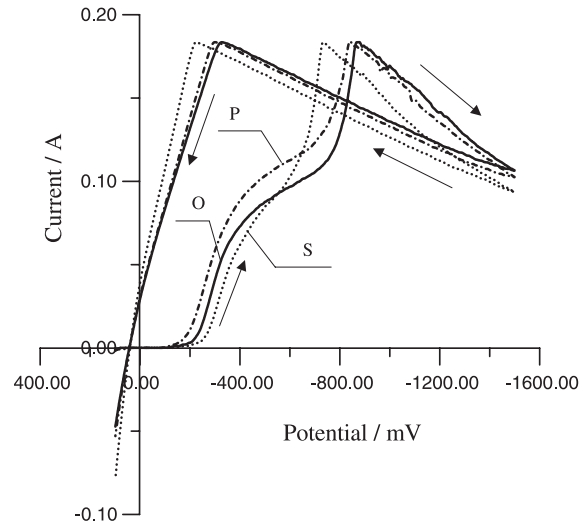


Fig. 4. Cyclic cathodic potentiodynamic polarization (CCPP) curves in the copper sulfate for the specimens anodically pretreated in 0.5 M oxalic acid (curve O) 3.0 M phosphoric acid (curve P) and 1.0 M sulfuric acid (curve S).

because the rate is too low, while powder-like deposits (with less adhesion) are produced at potentials  $< -0.600$  V. Upon the completion of the forward scan, for CCPP curves reaching  $-1.50$  V, all surfaces of the preanodized specimen were covered with a copper coating. OM observation verified this phenomenon.

Figure 5 shows the DP as a function of the acid concentration applied during pre-anodization. The DP shifts to more negative values as the acid concentration increases, especially from 0.25 to 1.5 M. This means that copper electroplating commenced at more negative potentials when the Al MMC was preanodized in more concentrated acids. For constant acid concentrations, the DP decreases in the order:  $P > O > S$ . This reflects the fact that Cu-plating commenced at less negative potentials (i.e., deposition starts earlier) when the Al MMC specimens were preanodized in phosphoric acid (P) rather than in oxalic (O) or sulfuric (S) acids.

In Figure 4, we find that the profile of the reverse scans in the current–potential diagram is quite similar regardless of which acid the Al MMC was preanodized in. The optical microscopic (OM) examination of the reverse scan, shows that copper electroplating was carried out onto a completely Cu-coated Al MMC surface. Consequently, the reverse scans correspond to the process where by Cu was electroplated onto a Cu-coated MMC. Thus the reverse scan profiles are similar, in spite of the different preanodizing treatments of the composites. The current density of the reverse scan increases gradually with less negative potentials, up to  $-0.200$  V, then suddenly decreases to zero at the cross-over potential (COP;  $+0.050$  V). At potentials more positive than the COP, the current becomes anodic, inducing copper dissolution.

In Figure 4, the difference between the DP and the COP is a measurement of the nucleation overpotential

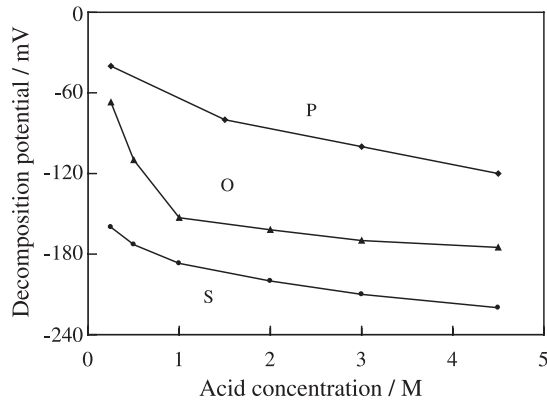


Fig. 5. DP as a function of acid concentrations in the formerly anodizing. P is for phosphoric acid, O for oxalic acid and S for sulfuric acid.

(NOP), which is responsible for copper coating nucleation [18, 19]. Figure 6 shows the variation of the NOP with the preanodizing acid concentration. The NOP varies with the kind of acid used and the concentration. The NOP estimated values, from Figure 6, are 0.146 V (in a 3.0 M phosphoric acid bath), 0.156 V (in a 0.5 M oxalic acid bath) and 0.233 V (in a 1.0 M sulfuric acid bath). The smaller the NOP the more feasible is the nucleation during copper plating. Hence, copper nucleation can more easily produced a refined copper deposit when the Al MMC has been preanodized in a 3.0 M phosphoric acid solution.

As shown in Figure 6, the NOP increases in the following order:  $P < O < S$  for a constant acid concentration and increases with increasing acid concentration. A fine-grained deposit formed at an NOP over 0.100 to 0.130 V [18, 19]. The NOP for Al MMC specimen preanodized in phosphoric acid was closed to this range, compared to specimens preanodized in other acids, thus resulting in a finer-grained copper coating.

### 3.6. EIS of preanodized specimens in a copper-plating bath

Electrochemical impedance spectroscopy (EIS) was used to investigate preanodized Al MMC specimens in copper-plating bath. The data are displayed as Bode plots ( $\log|Z|$  against  $\log f$ , and phase angle against  $\log f$ ,  $|Z|$  is the modulus of the impedance and  $f$  is the frequency). Bode plots are used because they provide more information over the entire frequency range than do Nyquist plots ( $-\text{Im } Z$  vs  $\text{Re } Z$ ,  $\text{Im } Z$  is the imaginary part and  $\text{Re } Z$  the real part of the impedance). Figure 7 shows a plot of the phase-angle against the frequency, from which we can see that, the resistive component  $R_f$  of the film produced during the preanodizing process can be evaluated for a frequency range between 0.1 and 50 Hz [20], and the capacitance  $C_f$  of the film can be estimated for frequency range between 300 and 20 000 Hz [20, 21]. The  $R_f$  data showed the following order: P (383  $\Omega$ ) > O (67  $\Omega$ ) > S (35  $\Omega$ ); the  $C_f$  data exhibited the order: P (144  $\mu\text{F}$ ) < O (565  $\mu\text{F}$ ) < S (4760  $\mu\text{F}$ ). In other words,

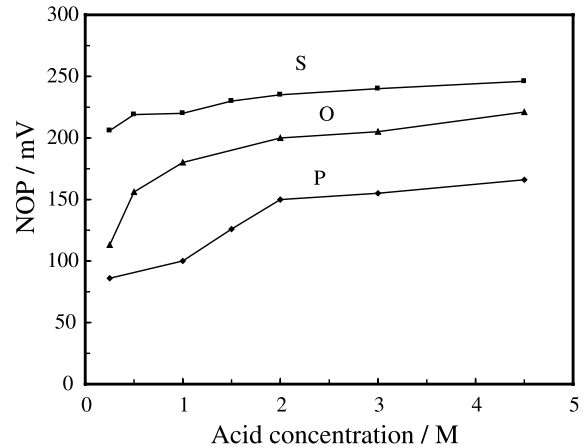


Fig. 6. Variation of the nucleation overpotential (NOP) with the concentration of the acids employed for formerly anodizing. P is for phosphoric acid, O for oxalic acid and S for sulfuric acid.

the specimens preanodized in phosphoric acid had the highest  $R_f$  (383  $\Omega$ ) but the lowest  $C_f$  (144  $\mu\text{F}$ ) while specimens preanodized in sulfuric acid had the lowest  $R_f$  (35  $\Omega$ ) but highest  $C_f$  (4760  $\mu\text{F}$ ), and those preanodized in O had medium  $R_f$  (67  $\Omega$ ) and  $C_f$  (565  $\mu\text{F}$ ). Figure 3 shows the morphology, revealing no wrinkled surface film in the continuous phase, for the highest  $R_f$  but lowest  $C_f$ , but there is a wrinkled film in the continuous phase, shown in Figure 3(c), associated with the lowest  $R_f$  and highest  $C_f$ .

### 3.7. Initiation and development of copper deposition on preanodized 7005Al/Al<sub>2</sub>O<sub>3(P)</sub> MMC specimens

Figure 8(a) depicts the surface morphology of composite specimens preanodized in a 3.0 M phosphoric acid bath before the copper electroplating process. The interior of the aluminium matrix shows not only pitting but also attacks around the particles boundaries. Figure 8(b) shows the morphology of the 7005 Al alloy specimens anodized in the same way. Intergranular attacks occurred on the anodized 7005 Al alloy.

During the copper electroplating process, it was found that the nucleation of the copper coating started at the surface imperfections on both the Al alloy and on the Al MMC specimens. After electroplating the copper at 50 A m<sup>-2</sup> for 60 s, it was found that copper ions had become embedded, initiating Cu-deposition along the boundary sites of the reinforcing particles and at pits in the Al MMC matrix (Figure 8(c)). On the other hand, copper coating nucleation started at the grain boundaries on the Al alloy matrix (Figure 8(d)). Figure 8(e) illustrates the growth of the copper coating with the prolongation of the electroplating process to 180 s. The growth of the deposits Cu was initiated at boundary and pitting sites, combining towards the reinforcing particles, and finally expanding to cover the entire surface of the Al matrix in the MMC specimens. In contrast, Cu-deposits grew from the grain boundaries towards the grain interiors in the Al alloy specimens (Figure 8(f)).

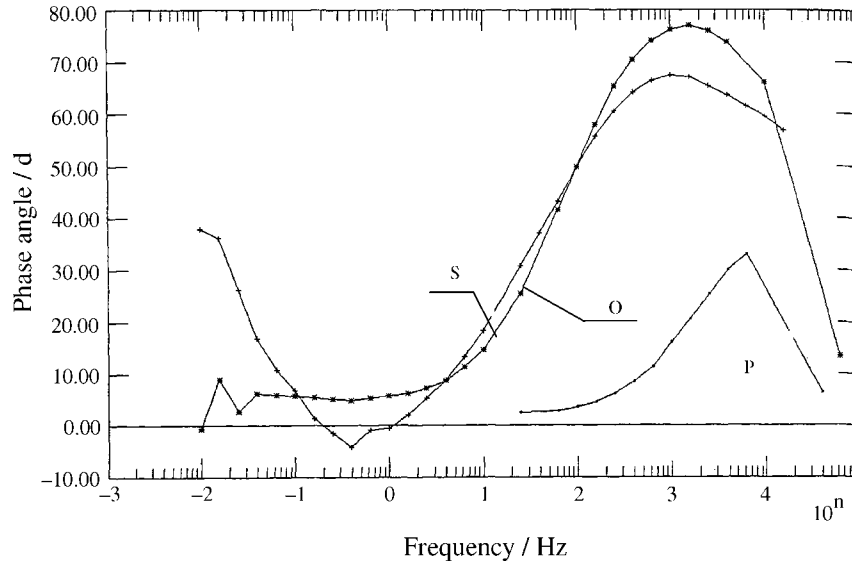


Fig. 7. Variation of phase angle with frequency for the specimens measured in the copper-electroplating bath. Curves B, P and S represent the specimens formerly anodized in 0.5 M oxalic acid, 3.0 M phosphoric acid and 1.0 M sulfuric acids, respectively.

## 4. Discussion

### 4.1. Films produced during various anodizing baths

The structure and properties of anodic films on aluminum substrates has been a subject of great interest [21–25]. It is believed [21–23] that anodic films that are a result of regular anodizing treatments comprise a compact inner barrier layer and a porous outer layer. Thompson et al. [21, 25] examined such films on aluminium substrates that had been anodized in various acids, by means of ultramicrotomy and ion beam thinning, to prepare samples for transmission electron microscopy (TEM), together with secondary ion mass spectrometry (SIMS). They found the inner layer to have a glassy or anion-free microcrystalline structure which had been produced as a result of the ionic migration of  $\text{Al}^{3+}$ ,  $\text{OH}^-$  and  $\text{O}^{2-}$ ; the outer layer was a microcrystalline acid anion-contaminated material that was deposited under the electric field from initially colloidal alumina [24]. They also found that the ratio of the thickness of the compact layer to the porous layer depended upon the kind of acids used in the anodizing process. The ratio increased in the following order: sulfuric acid (0.05/1) < oxalic acid (0.1/1) < phosphoric acid (0.5/1). On the basis of the ratios, the estimated relative thickness of the outer porous layer would decrease in the following order: sulfuric acid > oxalic acid > phosphoric acid. By checking the CAPP curves shown in Figure 2, it is found that the reverse scan current is greater than that the forward scan current in the case where the specimens were preanodized in a 3.0 M phosphoric acid bath. This means that the dissolution of the porous layer would prevail over its repair. When Al MMC was anodized at 1.200 V, in a 3.0 M phosphoric acid solution for 1 h, it is believed that almost all of the outer porous layer and the inner barrier

layer of the aluminum will be subjected to severe dissolution. This severe dissolution process leads to the neat appearance and shallow pits in the metal matrix, together with the boundary attack near the reinforcing phases, which is shown in Figure 3(a). If we examine curve O in Figure 2, we note that the reverse scan current is smaller than that the forward scan current. This means that the repairing of the porous layer will prevail over its dissolution when the specimen is anodized at 1.200 V in a 0.5 M oxalic acid solution for 1 h. As a result, the repaired porous layer becomes more compact, except at the boundaries around the reinforced phases, which are subject to attack, as shown in Figure 3(b). Curve S in Figure 2 shows that the currents in both the reverse and forward scans are similar. In this case, the dissolution of the porous layer has been compensated by the repair process when the specimen was anodized at 1.200 V in a 1.0 M sulfuric acid solution for 1 h. Thus, the thickness of the thick porous layer remained unchanged. This thick porous layer tended to shrink to form a wrinkled film during the drying process prior to SEM observation, as shown in Figure 3(c). The attack around the boundaries during reinforcing phases might be a result of sulfuric acid that had penetrated the films [20].

### 4.2. Behaviour of preanodized specimens in a copper sulfate electrolyte bath

The behaviour of the preanodized specimens in a copper sulfate solution is also of great interest. According to Thompson and Wood [21], the thickness of the inner barrier layers on preanodized aluminum samples submerged in various acids, decreases in the following order: phosphoric acid > oxalic acid > sulfuric acid, but the thickness for the outer porous layers increases in the following order: phosphoric acid < oxalic acid <

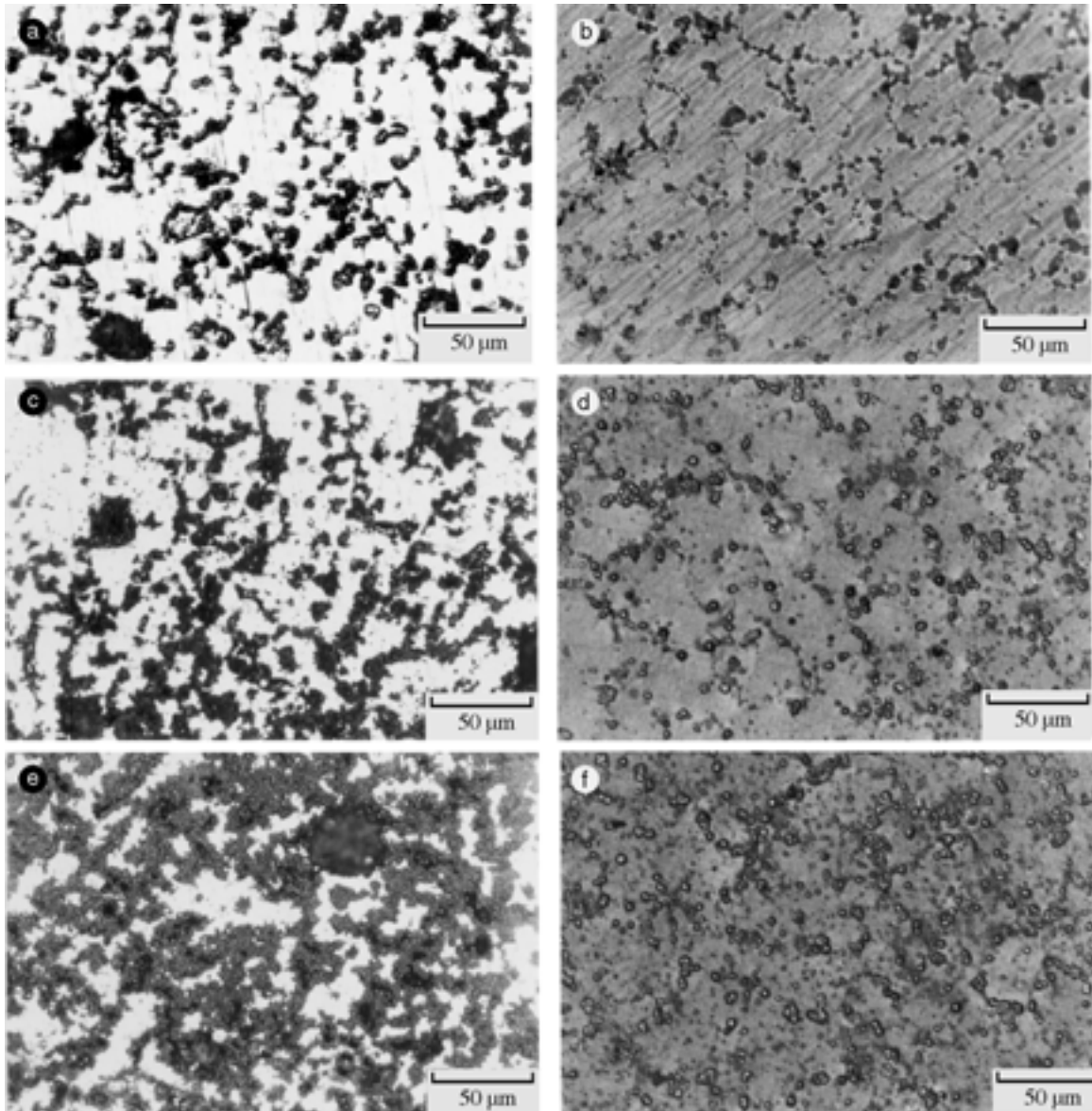


Fig. 8. Optical micrographs (OMs) for (a) 7005Al/Al<sub>2</sub>O<sub>3(p)</sub> MMC and (b) Al 7005 alloy anodized in 3.0 M phosphoric acid; (c) OM for the copper coat electroplated on 8(a) post plating at 50 A m<sup>-2</sup> for 60 s; (d) OM for the copper coat on 8(b) post plating at 50 A m<sup>-2</sup> for 60 s. (e) and (f) are similar to (c) and (d) but prolonging the time of electroplating to 180 s.

sulfuric acid. An EIS study of Al MMC samples subjected to a variety of preanodizing conditions was conducted by immersion in copper sulfate, to estimate the resistance ( $R_f$ ) and capacitance ( $C_f$ ) of the resultant films. The data in Section 3.6 indicates that  $R_f$  and  $C_f$  depend on the acid used in the preanodization process. The magnitude of  $R_f$  (in ohms) shows a trend similar to that of the thickness of the barrier layer, decreasing in the following order: phosphoric acid (383) > oxalic acid (67) > sulfuric acid (35). The magnitude of  $C_f$  (in  $\mu\text{F}$ ) shows a trend similar to the thickness of the porous layer, increasing in the following order: phosphoric acid (144) < oxalic acid (565) < sulfuric acid (4760). In other words, if immersed in copper sulfate, MMC specimens preanodized in phosphoric acid had a compact barrier layer, but those preanodized in sulfuric acid had a diffuse one.

The discussion thus far indicates that the Al MMC samples preanodized in phosphoric acid are covered with a thin compact layer, together with pits in the matrix, and boundary attacks along the reinforcing particles. The sites of the pits and boundary attacks even allow exposure of the metallic aluminium substrate allowing the embedding of copper ions, thus initiating nucleation. As a result, MMC specimens that had been preanodized in phosphoric acid possessed numerous surface nucleation sites. The development of these resulted in a fine-grained copper deposition, as shown in Figure 1(a).

In contrast, the Al MMC specimens that had been preanodized in oxalic acid were covered with a double film, predominantly due to a diffuse porous layer and a compact inner layer. It is conceivable that this double film hindered nucleation during copper electroplating.



Only a few sites were exposed for the embedding of copper ions. The development of such a limited number of nucleation sites led to a coarse-grained copper deposit, as shown in Figure 1(b). To some extent, the excessively diffuse porous film on the composite samples, preanodized in sulfuric acid, resulted in a large nodular copper coating (Figure 1(c)).

This inference can be confirmed by examination of the results in Figures 4, 5 and 6. According to Figure 4, the DP decreases in the following order: P > O > S. It is well known that the plating process occurs readily for systems with a DP at less negative potentials. Therefore, the ease of the commencement of the copper plating process decreases in the order: P > O > S. In Figure 5, the DP order also reveals that: P > O > S regardless of the acid concentration. In Figure 6, the NOP has the order: P < O < S in spite of the acid concentration. It is known that the smaller the NOP, the finer the grain of the deposits. In the present work, the NOP exceed the range between 0.100–0.150 V, which according to Lamping [18], is the optimal range for obtaining fine-grained copper deposition.

## 5. Conclusions

- (i) The electroplating of copper directly onto 7005Al/Al<sub>2</sub>O<sub>3(P)</sub> MMC (Al MMC) is difficult but becomes feasible once the Al MMC substrates have been preanodized in mineral acids.
- (ii) According to tape tests, classes 0 and 1 adhesion strengths are satisfactory, thus the corresponding electroplating processes are acceptable.
- (iii) Specimens preanodized in phosphoric acid performed better than those preanodized in oxalic or sulfuric acid, especially in a 3.0 M phosphoric acid bath at 1.200 V for 1 h.
- (iv) Electrochemical studies provided useful information that delineated the role of the preanodization of Al MMC specimens. The usefulness for Cu-electroplating can be estimated from the CCPP (cathodic cyclic potentiodynamic polarization) curves for MMC specimens preanodized in a copper sulfate solution.
- (v) During the electroplating process of the copper initially nucleated at pits in the matrix and at the phase boundaries of reinforced particles, these expanded

to cover the reinforcing particles, finally entirely coating the surface of the Al MMC specimens.

## Acknowledgement

The authors would like to thank the National Science Council of the Republic of China for financially supporting this research under contract NSC-88-2216-E-008-004.

## References

1. D.M. Aylor, 'Metal Handbooks', 9th edition, Vol. 13 (American Society for Metals, OH, 1987), p. 859.
2. P.K. Rohatgi, R. Astana and S. Das, *Int. Met. Rev.* **31** (1986) 115.
3. A.M. Patton, *J. Inst. Metals* **100** (1972) 197.
4. F.A. Lowenheim, 'Electroplating' (McGraw-Hill, New York, 1978), p. 188.
5. C.R. Smith, *US Patent 5, 730 853* (1998).
6. J-C. Lin and W-D. Jehng, 7th International Symposium on Electrochemical Methods in Corrosion Research, 28 May–1 June, 2000 Budapest, Hungary, No. 080, p. 128.
7. S. Kawai, H. Sato and T. Sakai, *US Patent 4, 109 287* (1978).
8. J-C. Lin, J-G. Her, S-B. Jiang, C-N. Chang and J-R. Your, *US Patent 6 187 461B1* (2001).
9. R.G. King, in 'Surface Treatment and Finishing of Aluminium' (Pergamon Press, 1988), pp. 34–46.
10. D.J. Schardein, *Plat. Surf. Finish.* **80** (1984) 64.
11. F.J. Monteiro M.A. Barbosa, D.R. Gabe and D.H. Ross, *Plat. Surf. Finish.* **76** (1989) 86.
12. D.S. Lashmore, *Plat. Surf. Finish.* **81** (1985) 36.
13. D. Pletcher and F.C. Walsh, 'Industrial Electrochemistry' (Blackie Academic & Professional, Glasgow, 1993), p. 389.
14. W-D. Jehng, Masters Thesis, Graduate Institute of Mechanical Engineering, National Central University, Chung-Li, Taiwan, ROC (June, 1997), p. 43.
15. D.C. Silverman, *Corrosion* **48** (1992) 735.
16. W.S. Tait, *Corrosion* **34** (1978) 214.
17. W.S. Tait, *Corrosion* **35** (1979) 296.
18. B.A. Lamping and T.J. O'Keefe, *Met. Trans.* **7B** (1976) 551.
19. J.C. Lin and S.L. Tsai, *J. Appl. Electrochem.* **24** (1994) 1044.
20. S. Lin, H. Greene, H. Shih and F. Mansfeld, *Corrosion* **48** (1992) 61.
21. G.E. Thompson and G.C. Wood, *Nature* **290** (1981) 230.
22. A.A. Mazhar, F.E. Heakal and K.M. Awad, *Thin Solid Films* **192** (1990) 193.
23. A.A. Mazhar, F. El-Taib Heakal and A.S. Mogoda, *Corrosion* **44** (1988) 354.
24. G.E. Thompson, R.C. Furneaux, G.C. Wood and R. Hutching, *J. Electrochem. Soc.* **125** (1978) 1480.
25. G.E. Thompson, R.C. Furneaux, G.C. Wood, J.A. Richardson and J.S. Goode, *Nature* **272** (1978) 433.